Composition and field-tuned magnetism and superconductivity in $Nd_{1-x}Ce_xCoIn_5$

Rongwei Hu,[1,2] Y. Lee,[3] J. Hudis,[4] V. F. Mitrovic,[2] and C. Petrovic[1]
[1]*Condensed Matter Physics, Brookhaven National Laboratory, Upton, New York 11973-5000, USA*
[2]*Physics Department, Brown University, Providence, Rhode Island 02912, USA*
[3]*Department of Earth System Sciences, Yonsei University, Seoul 120749, Republic of Korea*
[4]*Department of Physics and Astronomy, Johns Hopkins University, Baltimore, Maryland 21218, USA*
(Received 8 January 2008; revised manuscript received 24 March 2008; published 24 April 2008)

The $Nd_{1-x}Ce_xCoIn_5$ alloys evolve from local moment magnetism ($x=0$) to heavy fermion superconductivity ($x=1$). Magnetic order is observed over a broad range of x. For a substantial range of x ($0.83 \leq x \leq 0.95$) in the temperature-composition phase diagram we find that superconductivity may coexist with spin-density wave magnetic order at the Fermi surface. We show that a delicate balance betwen superconducting and magnetic instabilities can be reversibly tuned by both the Ce/Nd ratio and magnetic field, offering a unique model electronic system.

DOI: 10.1103/PhysRevB.77.165129 PACS number(s): 74.70.Tx, 71.27.+a, 75.30.Mb, 74.62.Bf

I. INTRODUCTION

In contrast to simple metals such as Pb, phase diagrams of unconventional superconductors often show a multitude of electronic phases of matter. In particular, magnetic order is ubiquitous in cuprate oxides and heavy fermion superconductor (HFSC) phase diagrams alike, as well as in some ruthenates and cobaltates. The proximity, competition, or coexistence of two distinct types of electronic order at the Fermi surface raised speculations that their driving mechanisms could be closely related.[1,2] Exotic superconductivity in heavy fermion materials[3] usually appears near the quantum critical point[4] where the magnetic ordering temperature is tuned to $T=0$ by a variety of external parameters. For example annealing, composition or magnetic field.[5] However, the most frequently used tuning parameter in HFSC is pressure.[6] This is in variance with the cuprate family where the interplay of superconductivity and magnetism is balanced by adjusting the in plane charge density of the CuO_2 layers. The discovery of pressure-induced superconductivity in $CeIn_3$ (Ref. 7) stimulated exploratory synthesis of $AuCu_3$ superstructures by Fisk, where the magnetic entropy might be further suppressed by crystallographic arguments.[8] Indeed, superconductivity in $CeRhIn_5$,[9] and $CeIrIn_5$,[10] was soon discovered, as well as the coexistence of heavy fermion superconductivity and magnetism in $CeRh_{1-x}Ir_xIn_5$.[11,12] $CeCoIn_5$,[13] the *primo* compound in the 115 family of HFSC, has also been recently hole doped to an antiferromagnetic ground state by Cd substitution on the In (1) site.[14] Despite a few examples of structurally tuned superconductivity in HFSC, the lack of a predictive theory suggests that there is still no clear understanding of how the delicate interplay of various degrees of freedom in these materials stabilizes superconducting, or a magnetic ground state.

The large quasiparticle mass enhancement in $CeCoIn_5$ is reflected in two large nearly cylindrical pieces of the Fermi surface and smaller 3D hole pockets.[15] Due to the pronounced $\vec{k}$-space inhomogeneity, hybridization of the $3d$ electrons of Co with the $5p$ electrons of In results in a small density of states at the Fermi energy, implying partially quasi-2D electronic structure.[16] By exploring a well defined nonhybridizing local moment such as Nd, we were able to continuously tune the coupling in the lattice and consequently quasiparticle mass enhancement between 4f ions and conduction electrons. As a result, we have obtained a rich phase diagram. The magnetic ground state in $Nd_{1-x}Ce_xCoIn_5$ smoothly evolves from local moment magnetism (LMM) on the Nd-rich side to HFSC on the Ce-rich side. Superconductivity coexists with other forms of electronic order, most likely magnetic in nature, in samples for Nd concentrations between $x=0.78$ and $x=0.98$. We demonstrate that the delicate balance between coexisting ordered states can be smoothly tuned by magnetic fields near the magnetic-superconducting boundary.

II. METHODS

Single crystals of $Nd_{1-x}Ce_xCoIn_5$ were grown from an excess In flux. Magnetic susceptibility, specific heat and resistivity measurements were performed in a Quantum Design MPMS XL 5 and PPMS-9 instruments, respectively. Single crystals were thoroughly ground to a fine powder for structural measurements. High resolution synchrotron powder x-ray patterns were taken at beamline X7A of National Synchrotron Light Source at Brookhaven National Laboratory. Monochromatic synchrotron x-ray and gas-proportional position-sensitive detector were used to measure the powder diffraction data. Rietveld refinements were performed using GSAS.[17] The samples were manually aligned to measure the magnetization, heat capacity, or resistivity for fields applied along the appropriate axis. M/H polycrystalline averages were calculated as $\chi(T)=[2\chi_{ab}(T)+\chi_c(T)/3]$ and were used to obtain the high temperature effective moments. Temperature dependent magnetic susceptibility was used to estimate the relative ratio of Ce/Nd ions. At high temperatures ranging from 150 K to 350 K, H/M curves were fit with Curie–Weiss (CW) law, $\chi(T)=C/(T-\Theta)$, where C is the Curie constant and Θ is the Weiss temperature. Electrical contacts for in-plane resistivity measurements were made with Epotek-H20E silver epoxy on thin platelike crystals whose dimensions were measured by optical microscope with 10 μm resolution. The samples were previously etched in diluted HCl

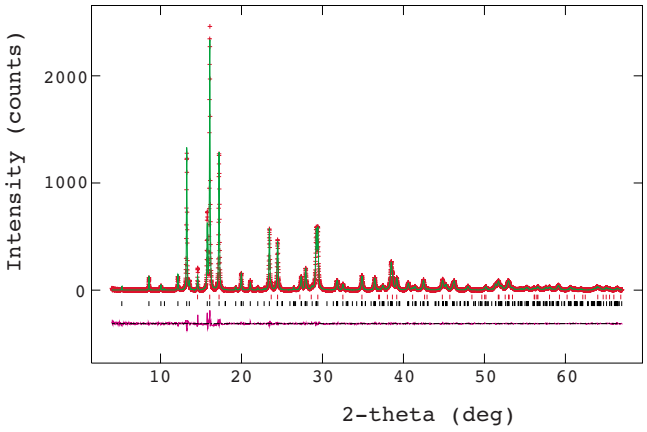

FIG. 1. (Color online) Synchrotron powder x-ray diffraction data of $Nd_{0.2}Ce_{0.8}CoIn_5$. For all x, only the $HoCoGa_5$ structure was detected, in addition to several small peaks of pure In from the flux.

for several hours and thoroughly rinsed in ethanol in order to remove excess In.

III. STRUCTURAL CHARACTERIZATION AND PHASE PURITY

Since both $NdCoIn_5$ and $CeCoIn_5$ are grown using identical temperature profiles and an identical ratio of starting materials Nd (Ce), Co and In,[13,18] one would expect a smooth change in the lattice parameters in the $Nd_{1-x}Ce_xCoIn_5$ alloy series.

Indeed, this is confirmed by high resolution structural measurements which showed that the samples crystallized in tetragonal $HoCoGa_5$ structure without any additional peaks introduced by Ce alloying (Fig. 1). Selected regions of the powder x-ray spectra showed monotonic evolution and uniform sharpness independent of x for both [111] and [003] peaks. This implies that Ce uniformly substitutes Nd with the increase in x and that our samples are indeed alloys rather than a mixture of intergrown compounds $NdCoIn_5$ and $CeCoIn_5$. The lattice parameters increase smoothly with Ce substitution in accordance with Vegard's law [Fig. 2(b)].

Magnetic susceptibility measurements did not detect magnetically ordered second phases, such as $NdIn_3$ or $CeIn_3$ (Fig. 3). The cubic compounds $CeIn_3$ and $NdIn_3$ order antiferromagnetically at 10 and 6.3 K, respectively.[7,19] Magnetic ordering in $NdCoIn_5$ is depressed smoothly with the increase in Ce, and we were able to follow the characteristic peak in M/H (signature of the onset of the magnetic order) down to lowest temperature of our magnetic measurement, $T=1.8$ K for $x=0.6$. Curie–Weiss analysis of polycrystalline magnetic susceptibility average at high temperatures showed at most a 4% deviation from the nominal ratio of Ce^{3+} and Nd^{3+} moments (Table I). As expected, the highest uncertainty in the nominal concentration of Ce(x) is in the middle of the alloy series, for the highest chemical disorder. Combined together, these results demonstrate that Ce uniformly substitutes Nd in the entire doping range of $Nd_{1-x}Ce_xCoIn_5$, with a maximum $\Delta x=0.04$.

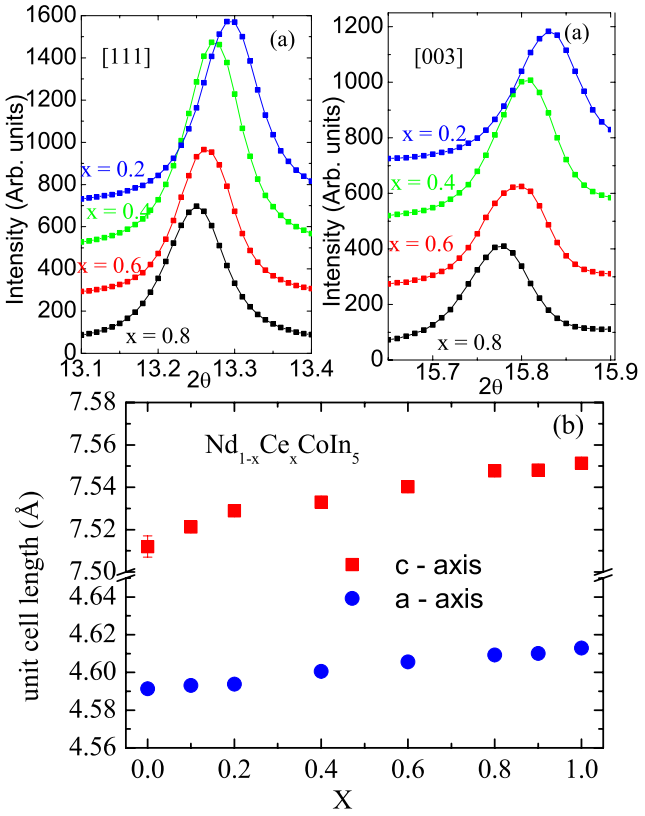

FIG. 2. (Color online) Selected regions of the synchrotron powder x-ray diffraction data for $Nd_{1-x}Ce_xCoIn_5$. Both [111] and [003] peaks shift uniformly with Ce substitution. (b) Tetragonal lattice parameters $\hat{a}$ (red symbols) and $\hat{c}$ (blue symbols)

IV. RESULTS

M/H data of $Nd_{1-x}Ce_xCoIn_5$ alloy series show substantial anisotropy (Fig. 3) at low temperatures and signature of magnetic order at $T_N=9$ K. For field applied along the $\hat{a}$-axis, $H\|\hat{a}$, the magnetic transition is rather broad. On the other hand, for $H\|\hat{c}$, the transition is relatively sharp implying complex magnetic order.

The thermodynamic properties of $Nd_{1-x}Ce_xCoIn_5$ are shown in Fig. 4. The magnetic ordering temperature in $NdCoIn_5$ is smoothly depressed from $T_N=9$ K with increased Ce concentration to 2.0 K by $x=0.6$ where $(C-C_{\text{latt}})/T$ shows a broad peak [Fig. 4(a)]. Interestingly, the magnetic ordering transition becomes sharper as x is further tuned toward the superconducting boundary for $x=0.7$. At $x\geq 0.78$ superconductivity emerges. With increasing x, the T_C increases to the bulk $T_C=2.3$ K of $CeCoIn_5$. The magnetic entropy released upon emergence of LMM [Fig. 4(a), inset] scales with Nd concentration up to $x=0.4$, implying that Ce ions do not play a direct part in the formation of the LMM ground state. In the HFSC state for $0.78\leq x\leq 1$, the magnetic entropy at 5 K is essentially invariant to changes in the Ce/Nd ratio. However, a hallmark of heavy fermion magnetism is observed for $x\geq 0.5$. This can be seen in the example of $x=0.6$ where only approximately $\sim 0.2\,R\ln 2$ is released below the magnetic ordering transition at 2 K. In the superconducting region at the Ce-rich side [Fig. 4(b)] addi-

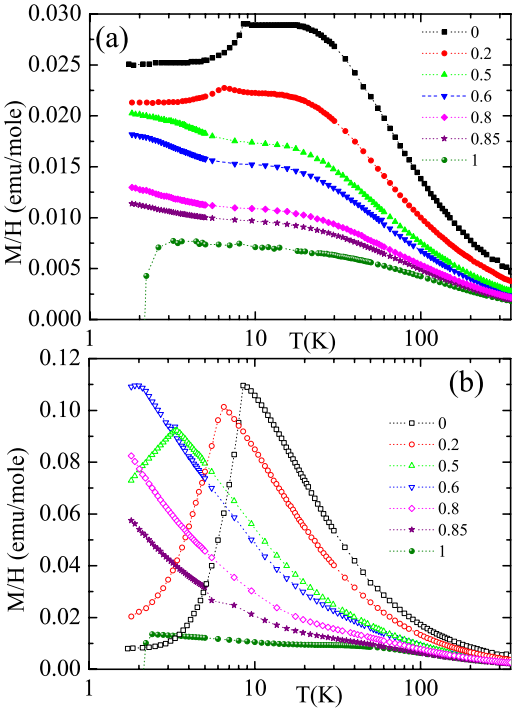

FIG. 3. (Color online) Magnetic properties of $Nd_{1-x}Ce_xCoIn_5$ alloy series in 1 kOe for (a) $H\uparrow\uparrow\hat{a}$ and (b) $H\uparrow\uparrow\hat{c}$ axis. Magnetic susceptibility shows decrease with Ce substitution, with easy axis along the crystalline $\hat{c}$ axis. The characteristic signature of antiferromagnetic order is observed down to $x=0.6$ above $T=1.8$ K for $\chi_C(T)$. The smooth evolution of $\chi_C(T)$ with x could indicate that magnetic fluctuation spectrum along the $\hat{c}$ axis is more relevant for tuning of the ground state.

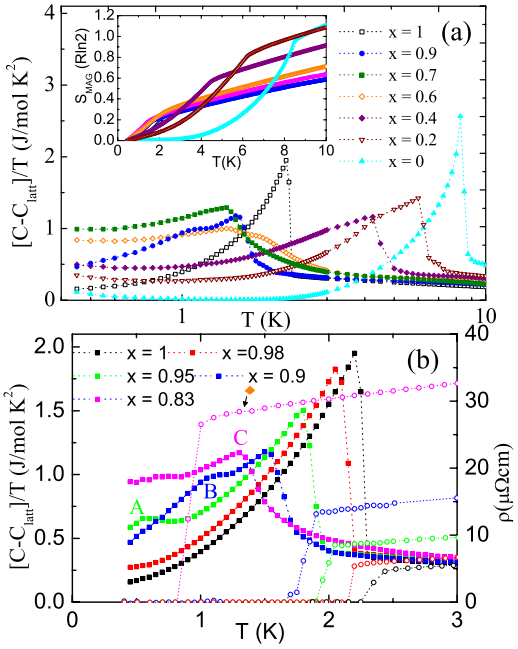

FIG. 4. (Color online) (a) Thermodynamic properties of $Nd_{1-x}Ce_xCoIn_5$. Specific heat of $LaCoIn_5$ was taken as the estimate of the lattice specific heat C_{latt}. Magnetic entropy (inset) obtained from integral $(C-C_{latt})/T$ in the same temperature range. (b) Thermodynamic and transport properties in the superconducting state, measured on the same sample for each Ce concentration x minus the lattice. The lattice resistivity was estimated by taking values of electrical resistivity of $LaCoIn_5$. With a decrease in the Ce/Nd ratio, the superconducting temperature T_C is suppressed. The additional thermodynamic anomaly increases in temperature $(A\rightarrow B\rightarrow C)$, as seen in the heat capacity data (full symbols). In-plane resistivity data (open symbols) are shown to identify superconducting transition.

tional thermodynamic anomalies A, B and C emerge in $(C-C_{latt})/T$ below the superconducting transition T_C for $x=0.95$, $x=0.9$, but above T_C for $x=0.83$.

By examining electronic transport we obtain further evidence for the presence of distinct types of electronic matter in the phase diagram. Temperature dependent electrical resistivities normalized to their value at 300 K [Figs. 5(a) and 5(b)] show a rather small loss of spin disorder scattering below Neel temperature in $NdCoIn_5$. This is consistent with the LMM-type of order in rare earth intermetallic compounds where local moments do not become part of Fermi surface upon cooling. By $x=0.5$ the electronic scattering strongly increases due to a single ion Kondo-type interaction and a logarithmic contribution of hybridizing Ce^{3+} ions submerged in the Fermi sea. Eventually for $x\geq 0.5$, a broad coherence peak develops in the lattice. This marks the emergence of an additional Kondo energy scale arising from the coherence in the heavy fermion lattice. As expected, the coherence temperature T_{COH} increases with the increase in Ce^{3+} ions. Looking from the Ce-rich side, the onset of the superconducting transition in $CeCoIn_5$ is depressed to 0.9 K and magnetic scattering increases by $x=0.83$ [Fig. 4(b)].

TABLE I. High temperature magnetic moment in $Nd_{1-x}Ce_xCoIn_5$ alloy series.

x	Measured μ_{eff} (μ_B)	Expected μ_{eff} (μ_B)	Error (%)
1	2.59(1)	2.54	2
0.85	2.67(6)	2.69	0.8
0.83	2.73(1)	2.71	0.8
0.8	2.72(1)	2.75	1
0.6	2.83(1)	2.96	4
0.5	2.96(1)	3.07	3
0.2	3.37(2)	3.40	0.8
1	3.7(1)	3.62	2

V. DISCUSSION

Heat capacity in the HFSC state for $x\leq 0.95$ reveals two thermodynamic anomalies. Only one $(C-C_{latt})/T$ discontinuity, though, corresponds to the superconducting transition [Fig. 4(b)]. One possible explanation for this would involve sample inhomogeneity and a distribution of the doping concentration. This, however, is very unlikely due to the low residual resistivity, the clean high resolution synchrotron powder x-ray diffraction pattern with uniform sharpness of

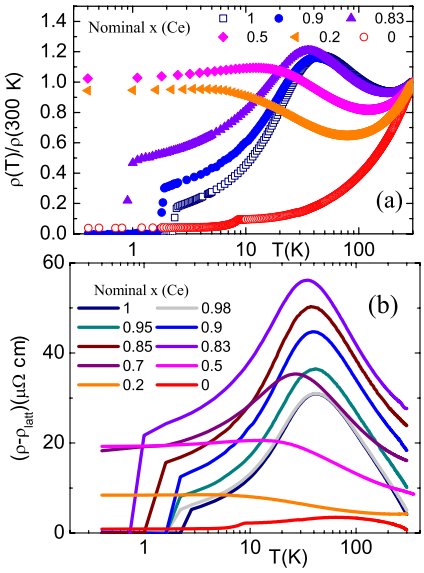

FIG. 5. (Color online) Results of resistivity measurements on $Nd_{1-x}Ce_xCoIn_5$ with current parallel to the [100]. (a) Resistivity curves normalized to their value at 300 K. (b) Magnetic contribution to the electrical resistivity $(\rho-\rho_{\text{lattice}})$. The lattice resistivity was estimated by taking values of electrical resistivity for $LaCoIn_5$.

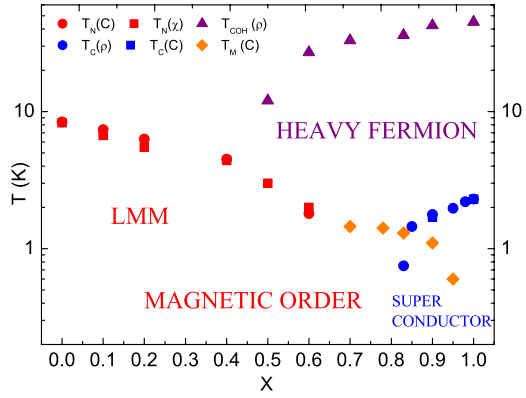

FIG. 6. (Color online) Phase diagram of $Nd_{1-x}Ce_xCoIn_5$ at $H=0$: superconducting T_C (blue symbols), antiferromagnetic Neel temperature (red symbols), coherence temperature of the Kondo lattice (purple symbols). Orange symbols represent second broad thermodynamic anomaly in C/T (below T_C) where resistivity shows small upturn (above T_C and for $x=0.7$ at $H=0$). The local moment antiferromagnetism of $NdCoIn_5$ smoothly changes to heavy fermion antiferromagnetic state around $x=0.5$. Magnetism and superconductivity meet around $x=0.8$. The Neel ordering temperature monotonically decreases for $0\leq x\leq 0.6$. For $x\geq 0.7$ heat capacity anomaly most likely corresponds to spin density wave type of magnetic order, deep in the superconducting state.

peaks for the whole range of x, and the compositional dependence of lattice parameters $\hat{a}$ and $\hat{b}$ in accordance with Vegard's law (Fig. 1). Furthermore, one would expect the highest degree of metallurgical disorder around the middle of the doping range, for $x=0.5$, and not near the Ce end. Finally, in superconducting materials with *metallic* type of bonding, metallurgical inhomogeneity would shift the bulk T_C of the *whole* sample, not only a fraction of the sample. For example, in $CeCu_{2.2}Si_2$ this is indeed seen in high resolution studies of the local structure.[20] Moreover, as seen in the heat capacity data for $x=0.1$, the two thermodynamic anomalies are comparable in size. Thus, secondary phases would have been easily detected in the analysis of powder x-ray spectra. Furthermore, as will be evident in Fig. 6, the smooth evolution of $T_C(x)$ and $T_M(x)$ argues against real space inhomogeneity. Our results imply that magnetic and superconducting phases coexist in the phase diagram, similarly to the situation in Cd-doping of $CeCoIn_5$.[14]

An alternative explanation involves two superconducting energy scales on different parts of the Fermi surface and negligible interband scattering. This could explain low temperature anomalies A and B for $x=0.95$ and $x=0.9$ since zero resistivity is achieved at the high temperature transition and is maintained through the low temperature transition. However, this scenario cannot explain thermodynamic anomaly C above the superconducting transition in $Nd_{0.17}Ce_{0.83}CoIn_5$ [Fig. 4(b)]. We speculate that low temperature discontinuities A and B, high temperature discontinuity C as well as sharp transition in $[C-C_{\text{latt}}]/T$ [Fig. 4(a)] for $x=0.7$ may be connected with some form of Fermi surface instability appearing concurrently on a different part of the Fermi surface. In what follows we show that this instability as well as the boundary between superconductivity and magnetism can be tuned by a magnetic field, in addition to composition x. Application of magnetic field reverses remarkable behavior seen with progressive decrease in the Ce/Nd ratio, tuning the boundary between the two ordered states.

The magnetic field depresses both T_C and B in $Nd_{0.9}Ce_{0.1}CoIn_5$ (Fig. 7). The suppression is rather anisotropic. For a field applied along the $\hat{c}$-axis superconducting anomaly in heat capacity and increasingly broad resistivity transition are suppressed to 0.5 K in 40 kOe. The anomaly B is observed only below 10 kOe, merging into a single thermodynamic transition for higher fields above 0.4 K, the lowest temperature of our measurement. On the other hand, for a field applied along $\hat{a}$-axis both thermodynamic anomalies show quite different field dependence. Superconducting T_C at 30 kOe, which is defined by the simultaneous onset of zero resistivity and the start of the heat capacity anomaly, is suppressed at 1.4 K. The anomaly B is observed below the T_C, just as we observe in $H=50$ kOe. In contrast to $H=0$ and $H=30$ kOe, zero resistivity in $H=50$ kOe corresponds to midpoint, rather than the onset of the heat capacity anomaly. In $H=70$ kOe, $Nd_{0.1}Ce_{0.9}CoIn_5$ electronic matter becomes equivalent to the $x=0.83$ sample at $H=0$ kOe: the main heat capacity transition is now above superconductivity. Electronic scattering for field applied in tetragonal plane [Fig. 3(b)] first increases and then decreases in the normal state as the magnetic field is tuned through $H_C=50$ kOe. The resistivity transition in $H\geq H_C$ is sharper implying a magnetic field induced phase transition for $H\uparrow\uparrow\hat{a}$-axis. The size of the superconducting anomaly in $(C-C_{\text{latt}})$ decreases in field relative to the size of additional thermodynamic anomaly B below T_C at $H=0$ for field applied along both crystalline axes. There is no loss of spin disorder scattering at the main heat capacity transition T_M for both $x=0.1$ samples in $H=70$ kOe [Fig. 7(b)] and for $x=0.83$ sample in $H=0$ [Fig.

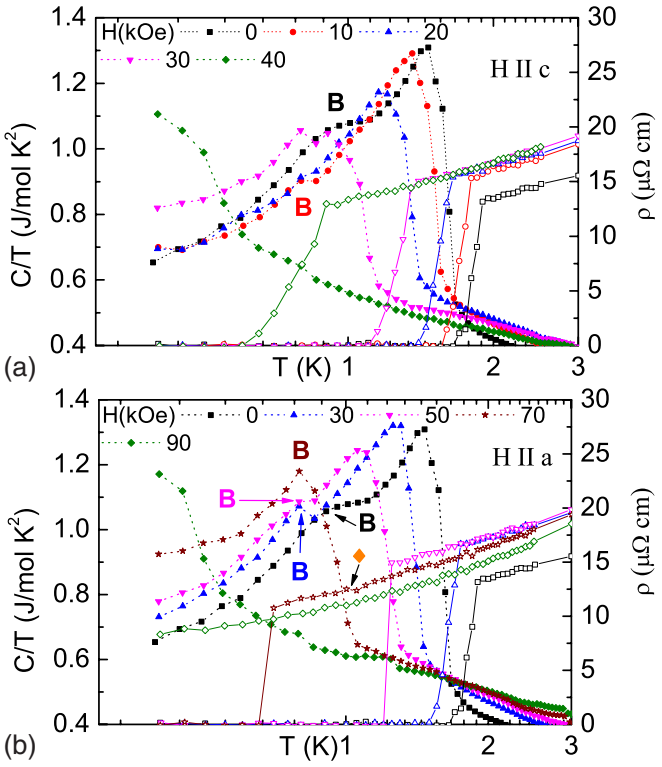

FIG. 7. (Color online) Thermodynamic and transport properties near magnetic-superconducting boundary, $x=0.1$, for $H\uparrow\uparrow\hat{c}$-axis (a) and $H\uparrow\uparrow\hat{a}$-axis (b). For each x, C/T and ρ data were taken from the same sample. The crossover from positive to negative magnetoresistance for $H\uparrow\uparrow\hat{a}$-axis suggests different nature of critical magnetic fluctuations below $H_C=50$ kOe and above H_C. Superconducting transition T_C corresponds to thermodynamic anomaly at higher temperature (below H_C) and at lower temperature (above H_C) for $H\uparrow\uparrow\hat{a}$-axis. A small feature in resistivity around 1 K for $H=70$ kOe could indicate opening of the partial gap at the Fermi surface in higher fields.

4(b)]. Instead, a very small upturn is observed in Fig. 4(b) ($x=0.83$, $H=0$) and in Fig. 7(b) ($x=0.1$, $H=70$ kOe) in resistivity (denoted by orange diamonds), a signature of the partial gapping of the Fermi surface. This is reminiscent of an itinerant spin-density-wave type-transition based on Fermi-surface nesting in a heavy-electron band observed in $Ce(Ru_{0.85}Rh_{0.15})_2Si_2$.[21]

It appears that $Nd_{1-x}Ce_xCoIn_5$ can support multiple electronic ordering states simultaneously. The coexistence of magnetism in superconductivity in Ce 115 superconductors has been induced by pressure in $CeRhIn_5$ or by composition in $CeRh_{1-x}Ir_xIn_5$, $CeCo(In_{1-x}Cd_x)_5$, and $CeRh_{1-x}Co_xIn_5$.[9,11,14,22] The low temperature specific heat and resistivity data taken in $Nd_{0.1}Ce_{0.9}CoIn_5$ at $H=0$ and in $Nd_{0.17}Ce_{0.83}CoIn_5$ at $H=70$ kOe imply that T_C and T_M involve instabilities at different parts of the Fermi surface. The balance between these states is tuned only by degree of hybridization in the Kondo lattice (Ce/Nd ratio) and by magnetic field. Although the presence of additional magnetic transition made it difficult to estimate accurate values for the electronic heat capacity coefficient γ, by taking $\gamma=[C-C_{\text{latt}}(T)]/T$ above T_C, we observe that the large jump at ambient pressure in the specific heat of $CeCoIn_5$ $\Delta C/C(T_C)=4.35$ is reduced as more Nd enters into the matrix. For $x=0.98$ we observe $\Delta C/C(T_C)=3.79$ and by $x=0.1$ this ratio decreases to 1.76. Nevertheless, our results may indicate a general trend that increased Nd concentration decreases electron-boson coupling strength.[23]

In the standard paradigm, the suppression of heavy fermion antiferromagnetic order leads to superconductivity around the quantum critical point.[24,25] One aspect of the reduced Ce/Nd ratio in the lattice is a negative pressure. Using the bulk modulus of $CeCoIn_5$ $B=76$ GPa,[26] we estimate that a rigid shift of the lattice parameters for $x=0.83$ and $x=0.9$ corresponds to 0.03 GPa of applied pressure. Given that $\Delta T_C=0.9$ K (50%) between these two concentrations, this result implies that chemical pressure effects are less relevant than electronic tuning through increased hybridization.[27] This result applies not only to the magnetic–superconducting boundary where the contribution is only up to 2%, but also to the whole range of x since changes in the ground state in $Nd_{1-x}Ce_xCoIn_5$ are far more dramatic than what was observed in pressure-induced changes in the ground state in $CeCoIn_5$.[27]

It would be instructive to compare our results with the reported coexistence of superconductivity and magnetism in $CeRhIn_5$ under high pressure and to field-induced magnetic order in the superconducting state of $La_{1.9}Sr_{0.1}CuO_4$.[28–30] In both materials, as well as in $CeCoIn_5$, there are nodes in the superconducting gap. Delicate balance between antiferromagnetic and superconducting coupling near a quantum phase transition is smoothly tuned by magnetic field, which generates field-induced vortices that suppress superconductivity and enhance magnetic correlations.[31,32] In addition to this, in $Nd_{1-x}Ce_xCoIn_5$ suppression of d-wave superconductivity is certainly influenced by disorder, as seen in the large increase in residual resistivity (Fig. 5).[33]

The evolution of superconducting $T_C(x)$ with the increase in Nd is similar to $Ce_{1-x}La_xCoIn_5$.[34,35] This is consistent with dominant potential scattering and insensitivity of T_C to magnetic configuration of the rare earth ion, as observed in $Ce_{1-x}R_xCoIn_5$.[36]

VI. CONCLUSION

In conclusion, we have reported on Nd substitution in $CeCoIn_5$. Nd substitution results in the rich phase diagram, controlled apparently only by Ce/Nd ratio, i.e., by the level of 4f-conduction electron coupling. The ground state of this alloy series evolves from LMM to HFSC state via magnetically ordered heavy fermion ground state. A small concentration of Nd (5%) induces magnetic order deep in the superconducting state. We have demonstrated magnetic field tuning of the delicate balance between superconducting and magnetic ground state at the magnetic-superconducting boundary. We invite further investigation into possible microscopic coexistence of magnetic and superconducting order parameters by NMR and neutron scattering measurements. The possible existence of short range order (spin glass) between local moment magnetism and heavy fermion superconductor near the middle of alloy series would offer a

model electronic system with a rich interplay of superconductivity and magnetism comparable to high-T_C cuprate oxide superconductors.

ACKNOWLEDGMENTS

We thank R. Prozorov, S. L. Bud'ko, P. C. Canfield, Johnpierre Paglione and Myron Strongin for useful communication. This work was carried out at the Brookhaven National Laboratory, which is operated for the U.S. Department of Energy by Brookhaven Science Associates (Contract No. DE-Ac02-98CH10886). This work was supported by the Office of Basic Energy Sciences of the U.S. Department of Energy.

[1] Z. Fisk and D. Pines, Nature (London) **394**, 22 (1998).
[2] E. Demler, W. Hanke, and S. C. Zhang, Rev. Mod. Phys. **76**, 909 (2004).
[3] Z. Fisk, D. W. Hess, C. J. Pethick, D. Pines, J. L. Smith, J. D. Thompson, and J. O. Willis, Science **239**, 33 (1988).
[4] T. Senthil, A. Vishwanath, L. Balents, S. Sachdev, and M. P. A. Fisher, Science **303**, 1490 (2004).
[5] O. Trovarelli, M. Weiden, R. Müller-Reisener, M. Gomez-Berisso, P. Gegenwart, M. Deppe, C. Geibel, J. G. Sereni, and F. Steglich, Phys. Rev. B **56**, 678 (1997).
[6] H. Q. Yuan, F. M. Grosche, M. Deppe, C. Geibel, G. Sparn, and F. Steglich, Science **302**, 2104 (2003).
[7] N. D. Mathur, F. M. Grosche, S. R. Julian, I. R. Walker, D. M. Freye, R. K. W. Haselwimmer, and G. G. Lonzarich, Nature (London) **394**, 39 (1988).
[8] Z. Fisk and G. Aeppli, Science **260**, 38 (1993).
[9] H. Hegger, C. Petrovic, E. G. Moshopoulou, M. F. Hundley, J. L. Sarrao, Z. Fisk, and J. D. Thompson, Phys. Rev. Lett. **84**, 4986 (2000).
[10] C. Petrovic, R. Movshovich, M. Jaime, P. G. Pagliuso, M. F. Hundley, J. L. Sarrao, Z. Fisk, and J. D. Thompson, Europhys. Lett. **53**, 354 (2001).
[11] P. G. Pagliuso, C. Petrovic, R. Movshovich, D. Hall, M. F. Hundley, J. L. Sarrao, J. D. Thompson, and Z. Fisk, Phys. Rev. B **64**, 100503(R) (2001).
[12] A. Llobet, A. D. Christianson, Wei Bao, J. S. Gardner, I. P. Swainson, J. W. Lynn, J.-M. Mignot, K. Prokes, P. G. Pagliuso, N. O. Moreno, J. L. Sarrao, J. D. Thompson, and A. H. Lacerda, Phys. Rev. Lett. **95**, 217002 (2005).
[13] C. Petrovic, P. G. Pagliuso, M. F. Hundley, R. Movshovich, J. L. Sarrao, J. D. Thompson, Z. Fisk, and P. Monthoux, J. Phys.: Condens. Matter **13**, L337 (2001).
[14] L. D. Pham, T. Park, S. Maquilon, J. D. Thompson, and Z. Fisk, Phys. Rev. Lett. **97**, 056404 (2006).
[15] R. Settai, H. Shishido, S. Ikeda, Y. Murakawa, M. Nakashima, D. Aoki, Y. Haga, H. Harima, and Y. Onuki, J. Phys.: Condens. Matter **13**, L627 (2001).
[16] R. Settai, T. Takeuchi, and Y. Ōnuki, J. Phys. Soc. Jpn. **76**, 051003 (2007).
[17] A. C. Larson and R. B. VonDreele, Los Alamos National Laboratory Report No. LAUR 86-748, 2000 (unpublished).
[18] J. Hudis, Rongwei Hu, C. L. Broholm, V. F. Mitrović, and C. Petrovic, J. Magn. Magn. Mater. **307**, 301 (2006).
[19] M. Amara, R. M. Galéra, P. Morin, T. Veres, and P. Burlet, J. Magn. Magn. Mater. **130**, 127 (1994).
[20] D. Louca, J. D. Thompson, J. M. Lawrence, R. Movshovich, C. Petrovic, J. L. Sarrao, and G. H. Kwei, Phys. Rev. B **61**, R14940 (2000).
[21] S. Murayama, C. Sekine, A. Yokoyanagi, K. Hoshi, and Y. Onuki, Phys. Rev. B **56**, 11092 (1997).
[22] V. S. Zapf, E. J. Freeman, E. D. Bauer, J. Petricka, C. Sirvent, N. A. Frederick, R. P. Dickey, and M. B. Maple, Phys. Rev. B **65**, 014506 (2001).
[23] Y. Bang and A. V. Balatsky, Phys. Rev. B **69**, 212504 (2004).
[24] A. J. Millis, Phys. Rev. B **48**, 7183 (1993).
[25] F. Steglich, B. Buschinger, P. Gegenwart, M. Lohmann, R. Helfrich, C. Langhammer, P. Hellmann, L. Donnevert, S. Thomas, A. Link, C. Geibel, M. Lang, G. Sparn, and W. Assmus, J. Phys.: Condens. Matter **8**, 9909 (1996).
[26] P. S. Normile, S. Heathman, M. Idiri, P. Boulet, J. Rebizant, F. Wastin, G. H. Lander, T. Le Bihan, and A. Lindbaum, Phys. Rev. B **72**, 184508 (2005).
[27] V. A. Sidorov, M. Nicklas, P. G. Pagliuso, J. L. Sarrao, Y. Bang, A. V. Balatsky, and J. D. Thompson, Phys. Rev. Lett. **89**, 157004 (2002).
[28] Tuson Park, F. Ronning, H. Q. Yuan, M. B. Salomon, R. Movshovich, J. L. Sarrao, and J. D. Thompson, Nature (London) **440**, 65 (2006).
[29] G. Knebel, D. Aoki, D. Braithwaite, B. Salce, and J. Flouquet, Phys. Rev. B **74**, 020501(R) (2006).
[30] B. Lake, H. M. Ronnow, N. B. Christensen, G. Aeppli, K. Lefmann, D. F. McMorrow, P. Vorderwisch, P. Smeibidl, N. Mangkorntong, T. Sasagawa, M. Nohara, H. Takagi, and T. E. Mason, Nature (London) **415**, 299 (2002).
[31] E. Demler, S. Sachdev, and Y. Zhang, Phys. Rev. Lett. **87**, 067202 (2001).
[32] Y. Zhang, E. Demler, and S. Sachdev, Phys. Rev. B **66**, 094501 (2002).
[33] A. V. Balatsky, I. Vekhter, and Jian-Xin Zhu, Rev. Mod. Phys. **78**, 373 (2006).
[34] C. Petrovic, S. L. Bud'ko, V. G. Kogan, and P. C. Canfield, Phys. Rev. B **66**, 054534 (2002).
[35] S. Nakatsuji, S. Yeo, L. Balicas, Z. Fisk, P. Schlottmann, P. G. Pagliuso, N. O. Moreno, J. L. Sarrao, and J. D. Thompson, Phys. Rev. Lett. **89**, 106402 (2002).
[36] Johnpierre Paglione, T. A. Sayles, P.-C. Ho, J. R. Jeffries, and M. B. Maple, Nat. Phys. **3**, 703 (2007).